RSC Advances

PAPER

View Article Online
View Journal | View Issue

Cite this: *RSC Adv.*, 2017, **7**, 39852

Synthesis of poly(*p*-phenylene) containing a rhodamine 6G derivative for the detection of Fe(III) in organic and aqueous media†

Ho Namgung, Jongho Kim, Youngjin Gwon and Taek Seung Lee *

A conjugated polymer (CP) of poly(*p*-phenylene) (PPP) containing rhodamine 6G (R6G) was synthesized by the Suzuki-coupling reaction, in which PPP acted as a blue-emitting energy donor and R6G acted as a ligand for Fe(III) as well as the energy acceptor for Förster resonance energy transfer (FRET). The spirolactam ring in R6G was nonfluorescent and colorless, but became open upon exposure to Fe(III) and readily absorbed the blue emission of the PPP backbone. As the polymer was exposed to Fe(III), the blue emission from PPP decreased and the red emission of the ring-opened R6G increased *via* FRET. The sensing of the polymer for Fe(III) in ethanolic solution was not successful, because of negligible FRET. In the solid state of the polymer, the distance between the main chain (PPP) and the side chain (R6G) was sufficiently decreased to enable the transfer of fluorescence energy. As a result, the film sensor could detect Fe(III) in an ethanol solution and a paper-based strip sensor could detect Fe(III) in an aqueous solution with a change in the fluorescence color. The cellulosic paper of the strip provided rapid detection and improved the limit of detection. From the changes in the fluorescence of the polymer sensor in the presence of Fe(III), the film and strip sensors could detect Fe(III) in any media. Moreover, the film could be regenerated for repeated use after treatment with ethylenediaminetetraacetic acid (EDTA).

Received 17th July 2017
Accepted 9th August 2017

DOI: 10.1039/c7ra07853f

rsc.li/rsc-advances

Introduction

The development of synthetic probes for the detection of metal cations has gained considerable attention, because of the crucial role of such probes in environmental and biological systems.[1–3] Among the various metal cations investigated, Fe(III) is a vital nutrient required for the survival of living cells. Indeed, all organisms have developed their own specific metabolisms to absorb and transport Fe(III). Also, the detection of Fe(III) is particularly important because it catalyzes chemical reactions that produce reactive oxygen species.[4–6] Although a number of fluorescent sensors capable of Fe(III) detection have been developed, almost of these sensors are based on fluorescence quenching mechanisms that rely on the paramagnetic nature of Fe(III).[7–11] In addition, most of the fluorescence "turn-on" or "emission shift-"based sensors have detected Fe(III) mainly in their solutions. As such, reports on solid-based Fe(III) sensors are rare,[12–14] emphasizing the importance of the development of Fe(III)-detecting protocols that exhibit high sensitivity and selectivity in the solid state, such as nanoparticles, films, and fibers.[15–17]

The use of the FRET mechanism to detect Fe(III) is highly demanding, because it can avoid quenching-based sensing, enabling ratiometric detection. FRET is a nonradiative energy transfer process between an excited donor fluorophore and an acceptor fluorophore through long-range dipole–dipole interactions.[18–21] In general, FRET-based CP sensors exhibit high sensitivity over small molecules, because the fluorescence of CP could be easily altered by minimal stimuli.[22–25] We designed a blue-emitting PPP (donor) containing R6G derivative (acceptor) for the FRET-based detection of Fe(III). Rhodamine derivatives are often used as fluorescent reagents because of their strong fluorescence and long wavelength emission.[26–28] The (ring-closed) R6G that contains a spirolactam ring is nonfluorescent and colorless, whereas its ring-opened amide analog exhibits strong fluorescence and a pink color. The spirolactam structure of R6G is easily converted to the ring-opened amide structure by external stimuli such as acid and metal ions.[29,30] Similarly, the interaction of Fe(III) with the spirolactam ring of R6G causes the ring-opened amide form, inducing noticeable changes in its color and fluorescence, which have been exploited as turn-on probes for the detection of Fe(III).[31–35]

Herein, we synthesized a PPP containing R6G (R6G–PPP) for the detection of Fe(III). Using the "emission shift" effect of R6G in the presence of Fe(III), the R6G–PPP was expected to detect a small quantity of Fe(III) *via* FRET from the backbone of PPP to

Organic and Optoelectronic Materials Laboratory, Department of Organic Materials Engineering, Chungnam National University, Daejeon 34134, Korea. E-mail: tslee@cnu.ac.kr

† Electronic supplementary information (ESI) available: Synthesis of monomers, UV-vis and emission spectra of R6G–PPP in the absence and presence of Fe(III), and comparison of detection performance with other works. See DOI: 10.1039/c7ra07853f

R6G in the side chain. The changes in the fluorescence color of R6G–PPP during the FRET process could be estimated with a ratio of the fluorescent intensity of donor (blue) and acceptor (red). For the practical use of the Fe(III) sensor, a solid-state sensor for Fe(III) should be developed, because solid-state sensors possess many advantages over conventional solution sensors, such as easy handling, reusability, and a simple fabrication method.[36–40] The paper-based R6G–PPP strip was useful for detecting Fe(III) in aqueous solution and exhibited a short response time. The strip sensor has an advantage in portable applications and can be easily separated from the analyte solution after the detection, providing reusability.

Experimental

Instrumentation

^{1}H and ^{13}C nuclear magnetic resonance (NMR) spectra were recorded on a Bruker DRX-300 spectrometer with tetramethylsilane as the internal standard (Korea Basic Science Institute). Elemental analysis (EA) was performed with an Elemental Analyzer EA 1108 (Fisons Instruments). Fourier transform-infra red (FT-IR) spectra were recorded on a Bruker Tensor 27 spectrometer. Ultraviolet-visible (UV-vis) absorption spectra were obtained with a PerkinElmer Lambda 35 spectrometer. Fluorescence spectra were recorded on a Varian Cary Eclipse fluorescence spectrometer equipped with a xenon flash lamp excitation source. The molecular weight of the polymer was determined by gel-permeation chromatography (GPC). Tetrahydrofuran (THF) was used as the eluent with a polystyrene standard, and GMHHR-M columns and a Bischoff Lambda 1000 detector were used.

Reagents and materials

All chemicals were purchased from Sigma-Aldrich and solvents were purchased from Samchun Chemicals. All reagents were used without further purification unless otherwise noted. 1,4-Bis(octyloxy) benzene (**1**), 1,4-dibromo-2,5-bis(octyloxy)benzene (**2**), 1,4-di(ethyl-4-oxy-butyrate)benzene (**3**), 1,4-dibromo-phenyl-2,5-dioxybutyric acid (**4**), and rhodamine 6G-ethylenediamine (**5**) were synthesized according to previously published methods.[41–43]

Synthesis of 6

4 (1 g, 2.28 mmol) was dissolved in DMF (40 mL) under argon atmosphere. 1-Ethyl-3-(3-dimethylaminopropyl)carbodiimide (EDC) (1.09 g, 5.7 mmol) was added to the solution and then the mixture was stirred at room temperature for 1 h. *N*-Hydroxysuccinimide (NHS, 0.92 g, 7.98 mmol) was added to the mixture and the mixture was stirred at room temperature. After 1 h stirring, **5** (2.60 g, 5.7 mmol) was added to the mixture and the mixture was stirred at room temperature for 24 h. After the reaction, the mixture was slowly added to water (200 mL) and the precipitate was isolated by filtration. The precipitate was purified by silica-gel column chromatography and dried in a vacuum oven. Yield: 1.45 g (45%). ^{1}H NMR ($CDCl_3$, 300 MHz) 8.0 (2H, s), 7.9 (2H, m) 7.48 (6H, m), 7.08 (2H, m), 6.34 (4H, s), 6.2 (4H, s), 3.5 (4H, s), 3.2 (8H, m), 3.0 (4H, m), 1.9 (12H, m), 1.7 (8H, s), 1.3 (24H, m) ppm. FT-IR (KBr pellet, cm^{-1}): 3388 (N–H), 2970–2870 (C–H), 1678 (C=O), 1635 (N–H), 1622 (C=C), 1517 (C=C), 1269 (aromatic C–H). Anal. calcd for $C_{70}H_{80}Br_2NO_8$: C, 63.63%; H, 6.10%; N, 8.48%. Found C, 64.36%; H, 6.14%; N, 9.06%.

Polymerization of R6G–PPP

2 (0.34 g, 0.68 mmol), **6** (0.1 g, 0.076 mmol) and 1,4-benzenediboronic acid bis(pincol) ester (0.26 g, 0.76 mmol) were dissolved in a mixture of THF containing aqueous 2 M potassium carbonate solution (3 mL) under argon atmosphere. After addition of tetrakis(triphenylphosphine) palladium(0) (0.0438 g, 0.0379 mmol), the mixture was refluxed for 30 h. The mixture was cooled and poured to methanol (300 mL). The precipitate was isolated by filtration. The polymer was washed with water, methanol, and acetone. The polymer was extracted with chloroform for 24 h in a Soxhlet apparatus to remove oligomers and catalyst residues and the solution was precipitated in *n*-hexane. Finally, a gray powder was obtained after drying under vacuum. Yield: 0.29 g (78%). ^{1}H NMR (300 MHz, $CDCl_3$) 7.7 (s), 7.4 (m), 7.1–6.9 (m), 6.3 (s), 6.1 (s), 3.9 (m), 3.5 (m), 3.3 (m), 2.9 (m), 2.2–2.0 (m), 1.7–1.6 (m), 1.3–1.1 (m) ppm. ^{13}C NMR ($CDCl_3$) 124.35, 72.70, 72.48, 72.27, 71.85, 64.90, 27.1, 24.96, 21.39, 17.94, 9.37 ppm. FT-IR (KBr pellet, cm^{-1}): 3418 (N–H), 2925–2850 (C–H), 1680 (C=O), 1487 (C=C), 1209 (aromatic C–H). Anal calcd For $C_{30.9}H_{42.4}N_{0.48}O_{2.4}$: C, 80.89%; H, 9.25%; N, 1.5%. Found: C, 78.39%; H, 9.06%; N, 1.51%.

Preparation of R6G–PPP film and sensing test

A film of R6G–PPP was prepared *via* spin-casting on a glass slide from a 1 wt% chloroform solution. Then the film was immersed in an ethanolic Fe(III) solution for 2 h and air-dried for 5 min. Changes in the fluorescence of the film were recorded with the fluorescence spectrometer.

Preparation of R6G–PPP strip and sensing test

A cellulosic filter paper (Advantec no. 2) with a diameter of 5 mm was immersed in a THF solution of R6G–PPP (0.01 mg mL^{-1}). After 30 s, the filter paper was removed from the solution and air-dried. The prepared R6G–PPP strip was immersed in the aqueous Fe(III) solution for 5 min and dried for 5 min (heating may be needed for fast drying). The changes in the fluorescence intensity of the R6G–PPP strip were then recorded with the fluorescence spectrometer.

Results and discussion

Rhodamine 6G-ethylene diamine **5** was synthesized by the reaction of R6G with ethylene diamine according to a previously published method.[43] Monomer **6** was synthesized *via* a conventional EDC–NHS coupling reaction between the carboxylic acid moiety of **4** and the amino group of **5** (Scheme S1†). For the polymerization of R6G–PPP, the Suzuki coupling of **2**, **6**, and 1,4-benzenediboronic acid bis(pinacol ester) was carried out in the presence of Pd(0) catalyst, as shown in Scheme 1. The

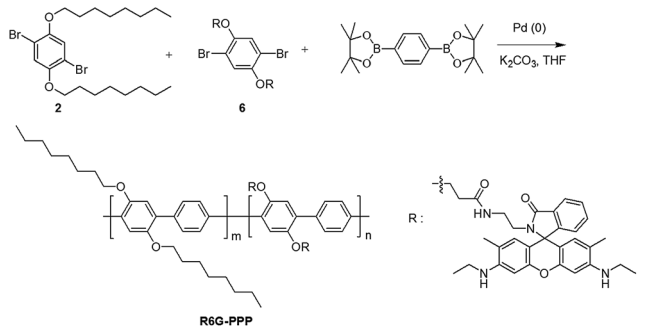

Scheme 1 Synthesis of R6G–PPP.

resulting R6G–PPP was soluble in common organic solvents, including chloroform and THF. The chemical structure of the polymer was confirmed by ^{1}H NMR, ^{13}C NMR, IR spectroscopy, and EA. The molar composition (m : n) of R6G–PPP was calculated to be 0.86 : 0.14 from the EA. GPC measurement indicated that the weight-average molecular weight of R6G–PPP was 11 270 with a polydispersity of 2.67. The UV-vis and fluorescence spectra of R6G–PPP were investigated in THF solution (0.01 mg mL^{-1}) and as a spin-cast film (Fig. S1†). The absorption wavelengths of R6G–PPP in THF solution and solid state were found to be at 348 and 354 nm, respectively. The emission wavelengths of R6G–PPP in both the solution and the solid were observed at 415 nm, emitting a blue fluorescence color (shown in the inset photographs in Fig. S1†).

The FRET-based detection mechanism of Fe(III) using R6G–PPP is illustrated in Scheme 2. When R6G–PPP is exposed to the Fe(III), R6G moiety, which is present in the side chain of R6G–PPP, will interact with Fe(III), resulting in the ring-opening, causing red fluorescence. Simultaneously, the blue emission of the phenylene backbone (energy donor) is transferred to the red emission of the R6G moiety (energy acceptor) through the FRET mechanism, leading to a red emission that is more intense than that excited at the absorption of R6G. To obtain FRET, the emission of the polymer backbone and the absorption of ring-opened structure of the R6G moiety should have a spectral overlap (Fig. S2a†). Upon exposure of R6G–PPP to Fe(III) in ethanol solution, the blue emission of R6G–PPP decreased, whereas the red emission increased (Fig. S2b†), indicating that the ring of the R6G moiety was opened by an interaction with Fe(III). However, the fully extended structure of the PPP backbone and the R6G side group in the solution might inhibit an efficient energy transfer. The fluorescent intensity at 560 nm of the R6G–PPP solution upon excitation at 525 nm (absorption of R6G) was more intense than that upon excitation at 348 nm (absorption of PPP), indicative of the poor energy transfer in the solution (Fig. S2c†). Thus, we sought the possibility of energy transfer in solid-state sensors such as a film and a paper-strip for detection of Fe(III) *via* FRET, because the distance between the PPP backbone and the R6G moiety would be sufficiently shorter in the solid state than in the solution state to obtain efficient FRET.

To enhance the sensitivity toward Fe(III) *via* FRET, R6G–PPP was fabricated into a spin-cast film on a glass substrate. The sensing procedure was simple; the R6G–PPP film was immersed in an ethanol solution of Fe(III) and the changes in UV-vis and fluorescence spectra were investigated. The changes in absorption and fluorescence of the film were monitored over various exposure times. Upon exposure to Fe(III), the absorption at 525 nm increased because of the ligand interactions between Fe(III) and R6G in the R6G–PPP, leading to ring-opening of the spirolactam in R6G (Fig. 1a). The blue emission (415 nm) of the PPP unit decreased and, concomitantly, the red emission (560 nm) of the R6G moiety increased because of FRET from PPP to the ring-opened R6G (Fig. 1b). The changes in fluorescence became saturated after immersion for 30 min (Fig. 1c), indicating that the interaction time between the two species was short enough for use as a sensory material. Moreover, the long wavelength (560 nm) emission intensity of the film was stronger when excited at the absorption of PPP unit (354 nm) than at 525 nm (Fig. 1d), indicating that efficient FRET was

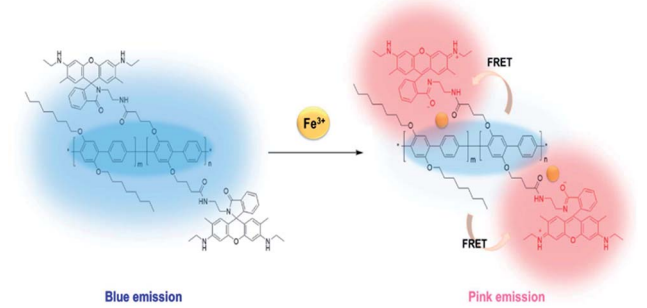

Scheme 2 FRET-based detection mechanism of Fe(III) using ring-opening of R6G–PPP.

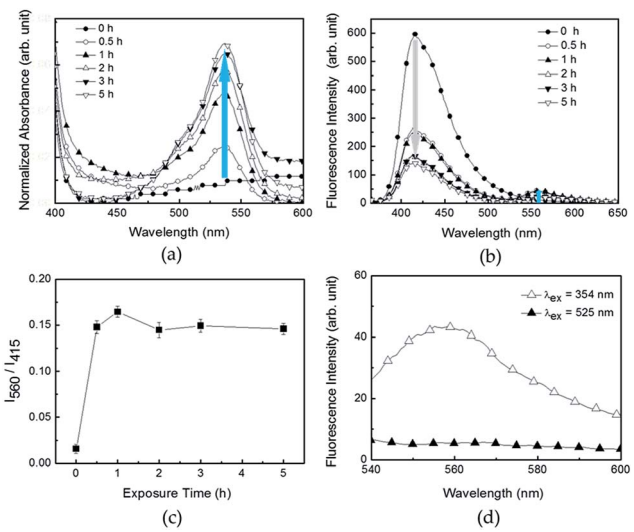

Fig. 1 Changes in (a) UV-vis and (b) fluorescence spectra of R6G–PPP film with exposure time in Fe(III) in ethanol solution (excitation wavelength λ_{ex} = 354 nm). (c) Relationship between fluorescence intensity ratio of acceptor and donor (I_{560}/I_{415}) in R6G–PPP film under various exposure times to Fe(III) solution. I_{560} and I_{415} correspond to fluorescence intensity at 560 nm and 415 nm, respectively. (d) Partial fluorescence spectra of R6G–PPP film upon exposure to Fe(III) excited at 354 nm (△) and 525 nm (▲). [Fe^{3+}] = 5.0 × 10^{-3} M.

accomplished in the film state, in contrast to the case in the ethanol solution.

Changes in the absorption and fluorescence properties of R6G–PPP film in the presence of various concentrations of Fe(III) are shown in Fig. 2. To see clear spectroscopic changes of the films, the exposure time was fixed to 2 h. Upon increasing the concentration of Fe(III) in an ethanolic solution (from 1.6×10^{-5} to 1.0×10^{-3} M), the absorption at 525 nm increased because of the ligand interactions (Fig. 2a). Similar to the fluorescence spectra of R6G–PPP in solution, the blue emission of the film decreased, while the red emission of rhodamine moiety increased (Fig. 2b). Such increase (560 nm) and decrease (415 nm) in each emission band was more intense when excited at the absorption of PPP (354 nm) *via* FRET than when excited at the absorption of the ring-opened R6G (525 nm) (Fig. 2c). The relative intensity ratio of I_{560}/I_{415} was highly dependent on the Fe(III) concentrations and the limit of detection (LOD) was calculated to be 4.14×10^{-4} M, based on the 3σ/slope, where σ is the standard deviation of four independent measurements (Fig. 2d). The concentration-dependent, fluorescence color change of R6G–PPP (blue-to-red) can be seen by the naked-eye (Fig. 2e). To test the reproducibility of the R6G–PPP film, EDTA was used to remove Fe(III) from the R6G–PPP film. After exposure to Fe(III), the R6G–PPP film exhibited red emission.

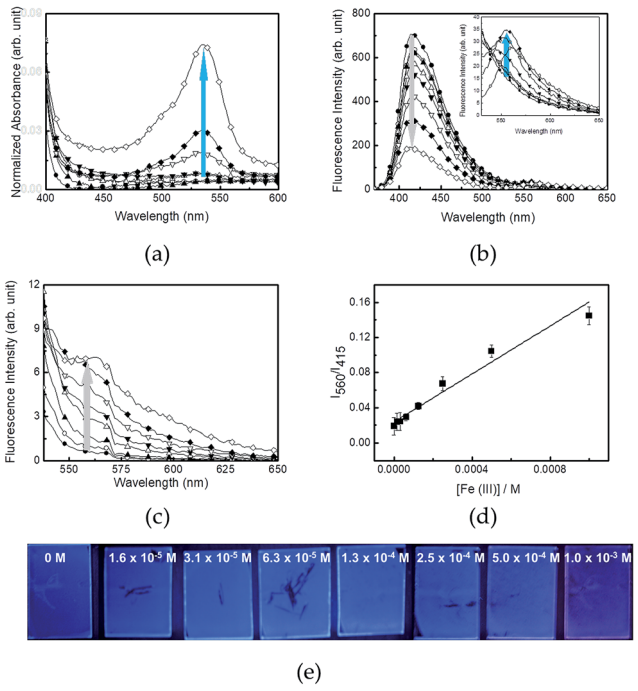

Fig. 2 Changes in UV-vis (a) and fluorescence spectra (b) and (c) of R6G–PPP film upon exposure to Fe(III) with various concentrations in ethanol solution (excitation wavelengths (b): 354 nm; (c): 525 nm). Inset corresponds to the partial fluorescence spectra. $[Fe^{3+}] = 0$ (●); 1.6×10^{-5} M (○); 3.1×10^{-5} M (▲); 6.3×10^{-5} M (△); 1.3×10^{-4} M (▼); 2.5×10^{-4} M (▽); 5.0×10^{-4} M (◆); 1.0×10^{-3} M (◇). (d) Relationship between fluorescence intensity ratio (I_{560}/I_{415}) of R6G–PPP film and concentration of Fe(III). (e) Photographs of R6G–PPP film under UV light (365 nm) before and after immersion in Fe(III) solution. Exposure time: 2 h.

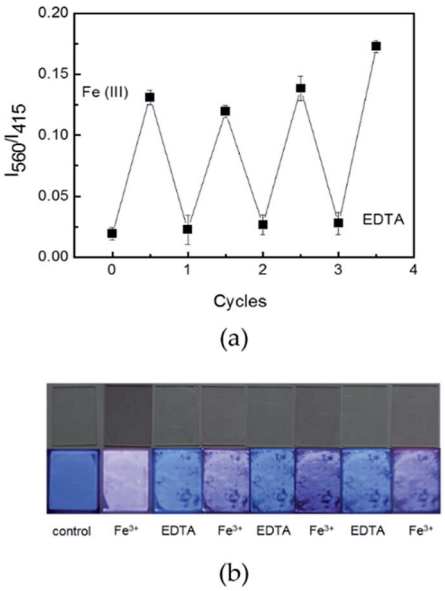

Fig. 3 Reversible regeneration of R6G–PPP film by EDTA. (a) Reversible change in the fluorescence intensity ratio (I_{560}/I_{415}) and (b) photographic images of R6G–PPP film in the presence of Fe(III) and EDTA under UV illumination (365 nm). The polymer film became stripped after continuous immersion in both solutions. Exposure time: 1 h. $[Fe^{3+}] = 5.0 \times 10^{-3}$ M; [EDTA] = 0.01 M; excitation wavelength $\lambda_{ex} = 354$ nm.

The red emission turned to blue again when the R6G–PPP film was immersed in an ethanolic EDTA solution. Fig. 3a shows the reproducible regeneration of the R6G–PPP film, indicating that the fluorescence intensity ratio I_{560}/I_{415} was reversibly changed

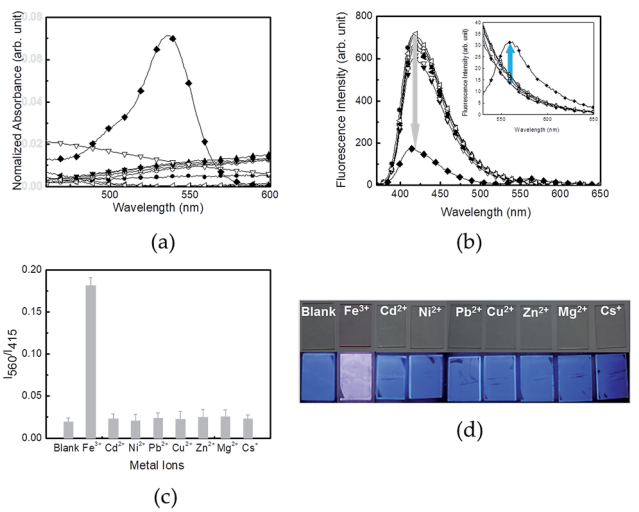

Fig. 4 Changes in (a) UV-vis and (b) fluorescence spectra of R6G–PPP film upon immersion in various metal-ion solutions. [Metal ions] = 5.0×10^{-3} M; excitation wavelength $\lambda_{ex} = 354$ nm; immersion time 1 h. Blank (●); Cs^+ (○); Mg^{2+} (▲); Zn^{2+} (△); Cu^{2+} (▼); Pb^{2+} (▽); Ni^{2+} (◀); Cd^{2+} (◁); Fe^{3+} (◆). The inset in (b) shows partial fluorescence spectra. (c) Comparison of the fluorescence intensity ratio (I_{560}/I_{415}) in the presence of various metal ions. (d) Photographic images of R6G–PPP film under ambient (upper) and 365 nm UV light (bottom) after immersion in various metal-ion solutions.

over four cycles. Such reversibility could be clearly observed by the naked-eye (Fig. 3b).

The selectivity of the R6G–PPP film toward various metal ions was investigated using absorption and fluorescence spectra. Among a series of cations, including Fe^{3+}, Cd^{2+}, Ni^{2+}, Pb^{2+}, Cu^{2+}, Zn^{2+}, Mg^{2+} and Cs^{+}, only Fe(III) rendered spectroscopic changes of the film (Fig. 4a and b). The increases in the absorption at 537 nm and in the intensity of fluorescence at 560 nm of the R6G–PPP film were observed upon exposure to Fe(III), and no spectroscopic change was found for the other metal ions, mainly because of the selective ring-opening of the spirolactam ring through the chelation of Fe(III) with the two oxygen atoms and two nitrogen atoms of the R6G side chain. Comparison of the fluorescence intensity ratio (I_{560}/I_{415}) showed that only Fe(III) was selectively bound to R6G–PPP to induce FRET (Fig. 4c). This phenomenon could be clearly observed by the naked-eye, in which pink color and red emission were seen under ambient and UV light (365 nm), respectively (Fig. 4d). Such immersion in a metal-ion solution has a practical problem when using the spin-cast film. Repeated exposure to the solution can strip the film from the substrate (as can be seen in Fig. 3b). Therefore, the dropping technique was used when exposing metal-ion solutions to the R6G–PPP film. Similar to the results obtained from the immersion technique, changes in the UV absorption and emission of the R6G–PPP film were observed (Fig. S3†).

To elucidate a more practical use of R6G–PPP in aqueous solution, R6G–PPP was introduced to a cellulose-based filter paper to prepare a sensor strip, which could avoid detachment from the substrate and provide a versatile use in aqueous solution. The use of such a strip sensor allowed changes in the fluorescence of R6G–PPP in the presence of Fe(III) in aqueous solution (Fig. 5a). Changes in the fluorescence of the R6G–PPP strip were observed and a decrease in the blue emission was accompanied by an increase in the red emission of R6G–PPP in the presence of Fe(III). Unexpectedly, such emission changes were completed within 1 min, which showed excellent sensitivity, compared with detection in solution or with film sensors, mainly because of the porous structure of the paper-based sensor strip (Fig. 5b). The changes in the fluorescence of the R6G–PPP strip in the presence of various concentrations of Fe(III) in water are shown in Fig. 6, where the sensor strip was

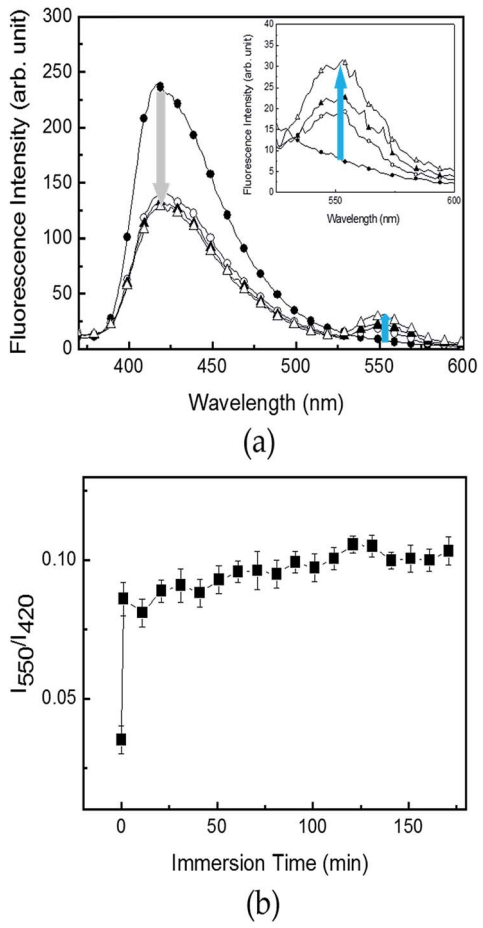

Fig. 5 (a) Changes in fluorescence spectra of R6G–PPP strip with immersion time in aqueous Fe(III) solutions. (Excitation wavelength $\lambda_{ex} = 354$ nm). The inset shows an enlargement of the fluorescence spectra. (b) Relationship between the acceptor/donor fluorescence intensity ratio (I_{550}/I_{415}) of R6G–PPP strip with immersion time. $[Fe^{3+}] = 0.01$ M.

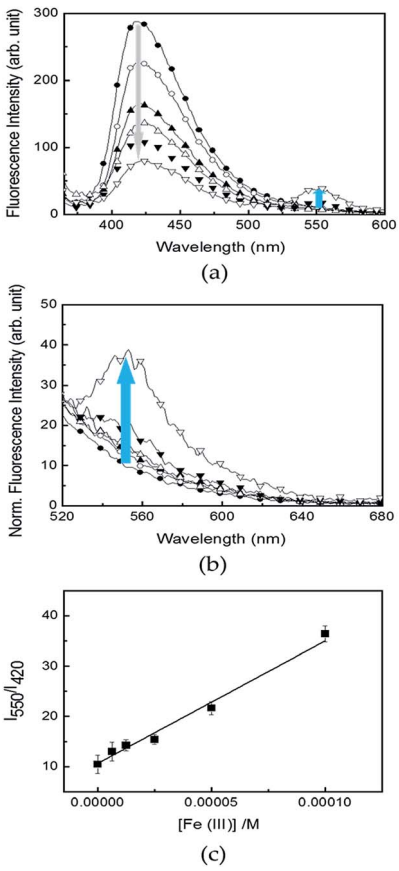

Fig. 6 Changes in fluorescence spectra of R6G–PPP strip in the presence of Fe(III) with various concentrations in aqueous solutions (a) and (b). Excitation wavelength $\lambda_{ex} = 354$ nm. (c) Relationship between the fluorescence intensity ratio (I_{550}/I_{415}) of R6G–PPP strip and Fe(III) concentrations. $[Fe^{3+}] = 0$ (●), 6.3×10^{-6} (○), 1.3×10^{-5} (▲), 2.5×10^{-5} (△), 5.0×10^{-5} (▼), and 1.0×10^{-4} M (▽). Exposure time: 5 min.

immersed only 5 min. Upon increasing the Fe(III) concentration (6.3×10^{-6} to 1.0×10^{-4} M), the decrease in the blue emission of the R6G–PPP strip was accompanied by an increase in the red emission *via* FRET (Fig. 6a and b). The intensity ratio (I_{550}/I_{415}) was linearly dependent on the concentration of Fe(III), and the LOD was found to be 1.0×10^{-6} M, which was enhanced compared with that of the R6G–PPP film (4.14×10^{-4} M) (Fig. 6c). Considering the solid-state sensor, the LOD of the paper-based R6G–PPP strip was comparable to other fluorescence-based Fe(III) sensors reported in literature (Table S1†).

Conclusions

R6G side chains were successfully introduced to a PPP backbone to use the ring-opening property of R6G in Fe(III) detection. Upon interaction of the R6G moiety with Fe(III), changes in the fluorescence of R6G–PPP were observed because of the spirolactam ring opening. Though the R6G–PPP showed a response to Fe(III) in solution, FRET-based emission amplification was negligible, presumably because of the extended distance between the polymer backbone (PPP) and the side chain (R6G), which rendered the energy transfer difficult. In the case of the solid state of R6G–PPP including film and paper-based strip, the FRET distance was sufficient to allow energy transfer to take place. Thus the R6G–PPP film exhibited better FRET-based detection performance toward Fe(III) including selectivity and reusability. The sensing of Fe(III) in the aqueous phase was also possible using a paper-based sensor strip with high sensitivity mainly because of its porous structure. As a result, R6G–PPP provided versatility as a Fe(III) sensor in organic and aqueous media.

Conflicts of interest

There are no conflicts to declare.

Acknowledgements

Financial support from the National Research Foundation of Korea (NRF) funded by Korean government through the Nuclear R&D Project (2015M2A7A1000217) is gratefully acknowledged.

Notes and references

1 A. Miyawaki, *Annu. Rev. Biochem.*, 2011, **80**, 357.
2 M. D. Best, H. Zhang and G. D. Prestwich, *Nat. Prod. Rep.*, 2010, **27**, 1403.
3 L. A. Finney and T. V. O'Halloran, *Science*, 2003, **300**, 931.
4 O. P. Lamba, D. Borchman and W. H. Garner, *Free Radical Biol. Med.*, 1994, **16**, 591.
5 H. Hiraishi, A. Terano, S. Ota, H. Mutoh, M. Razandi, T. Sugimoto and K. J. Ivey, *Am. J. Physiol.: Gastrointest. Liver Physiol.*, 1991, **260**, 556.
6 X. Huang, *Mutat. Res.*, 2003, **533**, 153.
7 A. Ananthanarayanan, X. Wang, P. Routh, B. Sana, S. Lim, D. Kim, K. Lim, J. Li and P. Chen, *Adv. Funct. Mater.*, 2014, **24**, 3021.
8 Y. Hu, B. Wang and Z. Su, *Polym. Int.*, 2008, **12**, 1343.
9 S. Ghosh, R. Chakrabarty and P. S. Mukherjee, *Inorg. Chem.*, 2009, **48**, 549.
10 L. Zhang, Q. Li, J. Zhou and L. Zhang, *Macromol. Chem. Phys.*, 2012, **213**, 1612.
11 R. Peng, F. Wang and Y. Sha, *Molecules*, 2007, **12**, 1191.
12 Y. Wei, Z. Aydin, Y. Zhang, Z. Liu and M. Guo, *ChemBioChem*, 2012, **13**, 1569.
13 A. J. Weerasinghe, C. Schmiesing, S. Varaganti, G. Ramakrishna and E. Sinn, *J. Phys. Chem. B*, 2010, **114**, 9413.
14 M. Shellaiah, Y. Wu, A. Singh, M. V. R. Raju and H. Lin, *J. Mater. Chem. A*, 2013, **1**, 1310.
15 C. Kaewtong, B. Wanno, Y. Uppa, N. Morakot, B. Pulpka and T. Tuntulani, *Dalton Trans.*, 2011, **40**, 12578.
16 Y. Liu, R. C. Mills, J. M. Boncella and K. S. Schanze, *Langmuir*, 2001, **17**, 7452.
17 Z. Guo, W. Zhu and H. Tian, *Macromolecules*, 2010, **43**, 739.
18 J. Bai, C. Liu, T. Yang, F. Wang and Z. Li, *Chem. Commun.*, 2013, **49**, 3887.
19 L. J. Fan, M. M. Hu, P. Shan and X. J. Peng, *Chem. Soc. Rev.*, 2013, **42**, 29.
20 F. He, Y. Tang, M. Yu, S. Wang, Y. Li and D. Zhu, *Adv. Funct. Mater.*, 2006, **16**, 91.
21 Y. Gao, M. Wei, X. Li, W. Xu, A. Ahiabu, J. Perdiz, Z. Liu and M. J. Serpe, *Macromol. Res.*, 2017, **25**, 513.
22 S. W. Thomas III, G. D. Joly and T. M. Swager, *Chem. Rev.*, 2007, **107**, 1339.
23 D. T. McQuade, A. E. Pullen and T. M. Swager, *Chem. Rev.*, 2000, **100**, 2537.
24 H. Namgung, C. Kim, Y. Kim, J. Kim and T. S. Lee, *J. Nanosci. Nanotechnol.*, 2016, **16**, 8805–8808.
25 Y. Wu, J. Li, L. Liang, D. Lu, J. Zhang, G. Mao, L. Zhou, X. Zhang, W. Tan, G. Shen and R. Yu, *Chem. Commun.*, 2014, **50**, 2040.
26 X. Q. Chen and J. Yoon, *Chem. Rev.*, 2012, **112**, 1910.
27 Y. Kim, G. Jang and T. S. Lee, *ACS Appl. Mater. Interfaces*, 2015, **7**, 15649–15657.
28 Y. Kim, H. Namgung and T. S. Lee, *Polym. Chem.*, 2016, **7**, 6655–6661.
29 V. Dujols, F. Ford and A. W. Czarnik, *J. Am. Chem. Soc.*, 1997, **119**, 7386.
30 Y. K. Yang, K. J. Yook and J. Tae, *J. Am. Chem. Soc.*, 2005, **127**, 16760.
31 M. H. Lee, T. V. Giap, S. H. Kim, Y. H. Lee, C. Kang and J. S. Kim, *Chem. Commun.*, 2010, **46**, 1407.
32 J. Li, Q. Hu, X. Yu, Y. Zeng, C. Cao, X. Liu, J. Guo and Z. Pan, *J. Fluoresc.*, 2011, **21**, 2005.
33 M. Chai, D. Zhang, M. Wang, H. Hong and Y. Ye, *Sens. Actuators, B*, 2012, **174**, 231.
34 N. R. Chereddy, K. Suman, P. S. Korraparti, S. Thennarasu and A. B. Mandal, *Dyes Pigm.*, 2012, **95**, 606.
35 V. Bhalla, N. Sharma, N. Kumar and M. Kumar, *Sens. Actuators, B*, 2013, **178**, 228.

36 L. Wang, W. Chen, W. Ma, L. Liu, W. Ma, Y. Zhao, Y. Zhu, L. Xu, H. Kuang and C. Xu, *Chem. Commun.*, 2011, **47**, 1574.
37 J. Hatai, S. Pal, G. P. Jose and S. Bandyopadhyay, *Inorg. Chem.*, 2012, **51**, 10129.
38 Y. Si, X. Wang, Y. Li, K. Chen, J. Wang, J. Yu, H. Wang and B. Ding, *J. Mater. Chem. A*, 2014, **2**, 645.
39 Y. J. Jin, J. H. Oh and G. Kwak, *Polymer*, 2016, **40**, 736.
40 G. Jang, J. Kim, D. Kim and T. S. Lee, *Polym. Chem.*, 2015, **6**, 714–720.
41 S. Sakthivel and T. Punniyamurthy, *Tetrahedron: Asymmetry*, 2012, **23**, 570.
42 T. Zhang, H. Fan, J. Zhou and Q. Jin, *J. Polym. Sci., Part A: Polym. Chem.*, 2009, **47**, 3056.
43 Y. Wang, H. Wu, J. Lio and X. Liu, *React. Funct. Polym.*, 2012, **72**, 169.